4. Shibuya H, Tsujii H. The structural characteristics of radiation oncology in Japan in 2003. *Int J Radiat Oncol Biol Phys* 2005;62:1472–1476.
5. Tanisada K, Teshima T, Ikeda H, *et al.* A preliminary outcome analysis of the Patterns of Care Study in Japan for esophageal cancer patients with special reference to age: Non-surgery group. *Int J Radiat Oncol Biol Phys* 2000;46: 1223–1233.
6. Tanisada K, Teshima T, Ohno Y, *et al.* Patterns of Care Study quantitative evaluation of the quality of radiotherapy in Japan. *Cancer* 2002;95:164–171.
7. Uno T, Sumi M, Sawa Y, *et al.* Process of care and preliminary outcome in limited-stage small-cell lung cancer: Results of the 1995–1997 Patterns of Care Study in Japan. *Int J Radiat Oncol Biol Phys* 2003;55:629–632.
8. Gomi K, Oguchi M, Hirokawa Y, *et al.* Process and preliminary outcome of a Patterns-of-Care Study of esophageal cancer in Japan: Patients treated with surgery and radiotherapy. *Int J Radiat Oncol Biol Phys* 2003;56:813–822.
9. Sugiyama H, Teshima T, Ohno Y, *et al.* The Patterns of Care Study and regional cancer registry for non–small-cell lung cancer in Japan. *Int J Radiat Oncol Biol Phys* 2003;56: 1005–1012.
10. Mitsumori M, Hiraoka M, Negoro Y, *et al.* The Patterns of Care Study for breast-conserving therapy in Japan: Analysis of process survey from 1995 to 1997. *Int J Radiat Oncol Biol Phys* 2005;62:1048–1054.
11. Teshima T, for the Japanese PCS Working Group. Patterns of Care Study in Japan. *Jpn J Clin Oncol* 2005;35:497–506.
12. SAS Institute Inc. SAS user's guide: statistics. Cary, NC: SAS Institute Inc.; 1985.
13. Oshima A, Kuroishi T, Tajima K, editors. Cancer statistics—2004. Tokyo: Shinohara Shuppan Shinsha; 2004. p. 207.
14. Statistics Bureau, Ministry of Internal Affairs and Communications. The 2005 population census, First basic complete tabulation. Available from: http://www.stat.go.jp/english/data/kokusei/2005/kihon1/00/hyodai.htm. Accessed May 17, 2007.
15. Parker RG, Bogardus CR, Hanks GE, *et al.* Radiation oncology in integrated cancer management: Report of the Inter-Society Council for Radiation Oncology. Merrifield, VA: American College of Radiology Publications, ISCRO; 1991.
16. Japanese PCS Working Group. Radiation oncology in multidisciplinary cancer therapy—Basic structure requirement for quality assurance of radiotherapy based on Patterns of Care Study in Japan, 2005. Self-publication supported by the Ministry of Health, Welfare and Labor in Japan.

Int. J. Radiation Oncology Biol. Phys., Vol. 72, No. 2, pp. 398–403, 2008

0360-3016/08/$–see front matter

ELSEVIER

doi:10.1016/j.ijrobp.2008.01.002

CLINICAL INVESTIGATION **Lung**

STEREOTACTIC BODY RADIOTHERAPY FOR OLIGOMETASTATIC LUNG TUMORS

YOSHIKI NORIHISA, M.D.,* YASUSHI NAGATA, M.D., PH.D.,* KENJI TAKAYAMA, M.D.,* YUKINORI MATSUO, M.D., PH.D.,* TAKASHI SAKAMOTO, M.D.,† MASATO SAKAMOTO, M.D.,‡ TAKASHI MIZOWAKI, M.D., PH.D.,* SHINSUKE YANO, B.S.,* AND MASAHIRO HIRAOKA, M.D., PH.D.*

*Department of Radiation Oncology and Image-Applied Therapy, Kyoto University Graduate School of Medicine, Kyoto, Japan; †Department of Radiation Oncology, Kumamoto University Graduate School of Medical Sciences, Kumamoto, Japan; and ‡Department of Radiology, Japanese Red Cross Society Wakayama Medical Center, Wakayama, Japan

Purpose: Since 1998, we have treated primary and oligometastatic lung tumors with stereotactic body radiotherapy (SBRT). The term "oligometastasis" is used to indicate a small number of metastases limited to an organ. We evaluated our clinical experience of SBRT for oligometastatic lung tumors.

Methods and Materials: A total of 34 patients with oligometastatic lung tumors were included in this study. The primary involved organs were the lung ($n = 15$), colorectum ($n = 9$), head and neck ($n = 5$), kidney ($n = 3$), breast ($n = 1$), and bone ($n = 1$). Five to seven, noncoplanar, static 6-MV photon beams were used to deliver 48 Gy ($n = 18$) or 60 Gy ($n = 16$) at the isocenter, with 12 Gy/fraction within 4–18 days (median, 12 days).

Results: The overall survival rate, local relapse-free rate, and progression-free rate at 2 years was 84.3%, 90.0%, and 34.8%, respectively. No local progression was observed in tumors irradiated with 60 Gy. SBRT-related pulmonary toxicities were observed in 4 (12%) Grade 2 cases and 1 (3%) Grade 3 case. Patients with a longer disease-free interval had a greater overall survival rate.

Conclusion: The clinical result of SBRT for oligometastatic lung tumors in our institute was comparable to that after surgical metastasectomy; thus, SBRT could be an effective treatment of pulmonary oligometastases. © **2008 Elsevier Inc.**

Stereotactic body radiotherapy, Metastatic lung tumor, Pulmonary metastases, Oligometastases.

INTRODUCTION

Stereotactic irradiation, stereotactic radiosurgery, and stereotactic radiotherapy are standard therapeutic techniques for intracranial tumors. With the introduction of three-dimensional localization techniques using a localizing frame of reference, hypofractionated irradiation using a stereotactic technique has been applied to extracranial tumors. Stereotactic body radiotherapy (SBRT) represents one of those treatments, and SBRT has been used in many institutes (1–9) mainly to irradiate lung or liver cancer.

Recently, patients with oligometastases, that is, a small number of metastatic lesions limited to an organ, have been considered candidates for curative treatment because long-term survival can be expected (10–13); therefore, surgical resection is the standard choice for patients with oligometastatic lung cancer. Since the effectiveness of SBRT for primary lung cancer was reported (5, 7, 14–17), awareness has been growing of SBRT as an effective option for curative treatment of lung tumors. In 1998, we began using SBRT for both primary and oligometastatic lung tumors. In this study, we retrospectively analyzed our experience with SBRT outcomes for oligometastatic lung tumors and reviewed the published data.

METHODS AND MATERIALS

Patient and tumor characteristics

The eligibility criteria of SBRT for oligometastatic lung tumor were as follows: *(1)* one or two pulmonary metastases, *(2)* tumor diameter ≤4 cm, *(3)* locally controlled primary tumor, and *(4)* no other metastatic sites. Of the patients treated between December 1998 and December 2004, 34 with oligometastatic lung tumors were included in this study. The primary involved organs were the lung ($n = 15$), colorectum ($n = 9$), head and neck ($n = 5$), kidney ($n = 3$), breast ($n = 1$), and bone ($n = 1$). Of these 34 patients, 25 were treated for

Reprint requests to: Yasushi Nagata, M.D., Ph.D., Department of Radiation Oncology and Image-Applied Therapy, Kyoto University Graduate School of Medicine, 54 Shogoin-Kawahara-Cho, Sakyo-Ku, Kyoto 606-8507, Japan. Tel: (+81) 75-751-3762; Fax: (+81) 75-751-3418; E-mail: nag@kuhp.kyoto-u.ac.jp

Supported by Grant-in-Aid H18-014 from the Ministry of Health, Labour and Welfare, Japan and Grant-in-Aid 18390333 from the Ministry of Education and Science, Japan.

Presented in part at the 46th Annual Meeting of the American Society for Therapeutic Radiology and Oncology (ASTRO), Atlanta, GA, October 3–7, 2004.

Conflict of interest: none.

Received Feb 5, 2007, and in revised form Dec 27, 2007. Accepted for publication Jan 3, 2008.

a single pulmonary nodule and 9 for two lesions. The histologic diagnosis of the primary disease was adenocarcinoma in 22, squamous cell carcinoma in 5, renal cell carcinoma in 3, adenoid cystic carcinoma in 2, pleomorphic carcinoma in 1, and osteosarcoma in 1 patient. Lung metastases were diagnosed clinically according to repeated thoracic computed tomography (CT) findings. Most patients had previously undergone surgical resection and chemotherapy for their primary cancer. Adjuvant oral chemotherapy regimens after SBRT were allowed. The patient characteristics are given in Table 1.

SBRT procedure

We used a combined X-ray and CT simulator—an integrated system using the same couch for the X-ray and CT simulators (Shimadzu, Kyoto, Japan). The patients were fixed in the stereotactic body frame (ELEKTA AB, Stockholm, Sweden) while CT scanning was performed with a slow scan time (4 s/slice).

Three-dimensional RT planning was performed using a treatment-planning machine (CADPLAN, version 3.1, and Eclipse, version 7.1, Varian Medical Systems, Palo Alto, CA). The internal target volume (ITV) was delineated on the CT images, considering the tumor motion assessed by X-ray fluoroscopy, and then the essential margins—planning target volume (PTV) margin and leaf margins—were added to the ITV (18, 19). We added 5 mm to the ITV for the PTV margin and another 5 mm from the contour of the PTV to the edge of the multileaf collimator for penumbra; thus, typically, a 10-mm margin was used between the contour of the ITV and the edge of the multileaf collimator. We used five to seven noncoplanar, static 6-MV photon beams and irradiated 12 Gy in each fraction at the isocenter. The patients received four or five fractions; therefore, the total dose was 48 Gy or 60 Gy at the isocenter within 4–18 days (median, 12 days).

Because we experienced several local failures with 48 Gy, the prescribed dose was escalated to 60 Gy from January 2001. However, the dose for metastases from primary lung cancer was maintained at 48 Gy because of difficulties in distinguishing a second primary lung cancer from a metastatic lesion and because the 5-year local relapse-free rate of 95% using this dose (16) was satisfactory. Also, the general pulmonary function was better in patients with metastatic lung cancer than in those with primary lung cancer. With the exception of patients with poor pulmonary function, a total dose of 60 Gy was prescribed to patients with a primary cancer other than lung cancer.

Table 1. Patient characteristics

Characteristic	Value
Patients (*n*)	34
Gender (*n*)	
Male	22
Female	12
Age (y)	
Range	30–80
Median	71
Performance status	
0	23
1	9
2	2
3–5	0
Primary tumor	
Lung	15
Colorectum	9
Head and neck	5
Kidney (renal cell carcinoma)	3
Bone (osteosarcoma)	1
Breast	1

Evaluation

The local response was assessed using the Response Evaluation Criteria in Solid Tumors and categorized into four types: *(1)* the disappearance of all target lesions (complete response), *(2)* at least a 30% decrease in the sum of the longest diameter of the target lesions (partial response), *(3)* a response ranging from a 30% decrease to a 20% increase in the sum of the longest diameter of the target lesions (stable disease), and *(4)* a ≥20% increase in the sum of the longest diameter of the target lesions (progressive disease). Because of the presence of consolidation with unclear margins around the tumor (20), it can be difficult to distinguish between tumor regrowth and radiation-induced injury; such cases were categorized as stable disease until apparent tumor regrowth was detected by careful and appropriate clinical observation for several months.

Survival was calculated from the first day of RT to the last day of follow-up. For overall survival, lost patients with clinically progressive disease and those with the terminal stage of disease were censored as dead. Adverse events were classified according to the Common Terminology Criteria for Adverse Events, version 3.

Statistical calculations were performed using Prism, version 4, software (GraphPad Software, San Diego, CA). The survival rates were analyzed using the Kaplan-Meier method, and differences in their distributions were evaluated using the log–rank test.

RESULTS

The study population comprised 22 men and 12 women, with median age of 71 years (range, 30–80 years). Of these 34 patients, 17 received 48 Gy in four fractions and 16 received 60 Gy in five fractions. One patient received 48 Gy in five fractions because of poor pulmonary function that necessitated a reduction in the fractional dose. The overall treatment time was 4–14 days (median, 12 days), except for

Table 2. Treatment results

Variable	Value
Tumor total (*n*)	43
Tumor diameter (*n*)	
<15 mm	17
≥15 but ≤30 mm	22
>30 mm	4
Prescribed dose (Gy)	
48	18
60	16
Overall treatment time (d)	
Range	4–18
Median	12
Follow-up period (mo)	
Range	10–80
Median	27

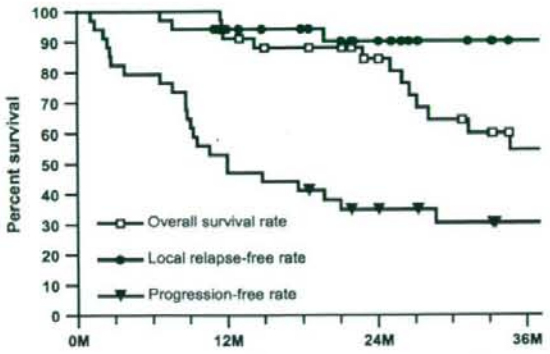

Fig. 1. Overall survival, local relapse-free survival, and progression-free survival rates after stereotactic body radiotherapy for oligometastatic lung cancer.

1 patient, for whom it was 18 days. The median follow-up period was 27 months (range, 10–80 months; Table 2).

Response

The overall survival rate, local relapse-free rate, and progression-free rate at 2 years was 84.3%, 90.0%, and 34.8%, respectively (Fig. 1). The numbers of patients with a complete response, partial response, stable disease, and progressive disease was 5, 8, 18, and 3, respectively. No statistically significant difference was found between those receiving 60 Gy and those receiving 48 Gy in terms of overall survival (p = 0.192; Fig. 2a); however, a marginally significant difference was observed between those receiving 60 Gy and 48 Gy in local progression-free survival (p = 0.078; Fig. 2b). No local progression was observed in tumors irradiated to 60 Gy, but three had local progression at 48 Gy. No differences were found in overall survival between patients with metastases from lung cancer and those with metastases from other cancers (p = 0.75).

Patterns of failure

Disease progression was observed in 23 patients (Table 3). Regrowth of the target lesions of SBRT was observed in 3 patients and recurrence of the primary lesion in 2. New metastatic lesions were observed in 19 patients. New intrapulmonary metastases were observed in 9 patients, and mediastinal or hilar regional lymph nodal metastases developed in 6. Distant metastases were observed in 3 patients: the adrenal gland in 2 and the liver in 1. One patient was diagnosed with progressive disease because of elevations of carcinoembryonic antigen and underwent chemotherapy.

Toxicity

The adverse events resulting from SBRT were classified using the Common Terminology Criteria for Adverse Events, version 3 (Table 4). Pulmonary toxicity was observed as cough, hemosputum, dyspnea, pleural effusion, and radiographic changes and was Grade 1 in 23 patients (68%) and Grade 2 in 4 (12%). One patient required oxygen

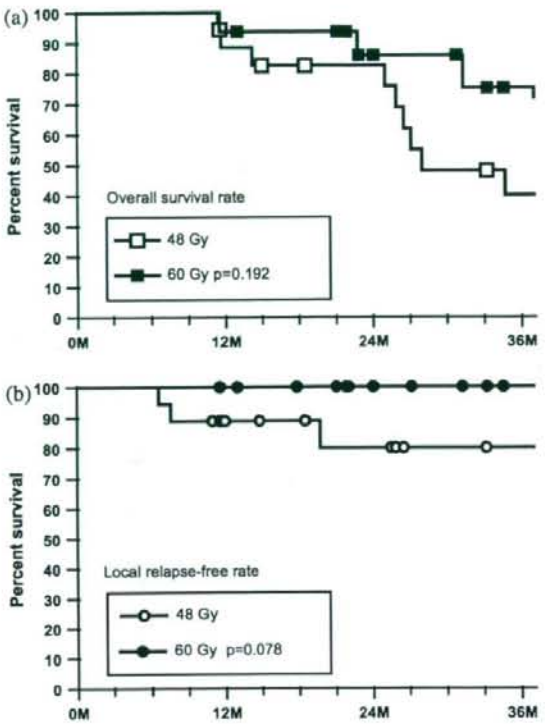

Fig. 2. (a) Overall survival rates of patients treated with 48 Gy and 60 Gy. (b) Local relapse-free rates of patients treated with 48 Gy and 60 Gy. Difference was marginally significant (p = 0.078).

supplementation for bacterial pneumonia 18 months after SBRT and was considered to have Grade 3 pulmonary toxicity. The symptoms of most patients were mild and did not interfere with their activities of daily living. Grade 1 skin toxicity with faint erythema or pigmentation with or without symptoms was observed in 6 patients (17%). One patient had a skin ulcer at the site of the reirradiated field, contralateral to the site of SBRT, and was cured with conservative treatment. Musculoskeletal adverse events were

Table 3. Patterns of disease progression

Pattern	*n*
New pulmonary metastasis	9
Regional lymph node metastasis	6
Local regrowth of target lesion of SBRT	3
Recurrence of primary lesion	2
Adrenal gland metastasis	2
Liver metastasis	1
Tumor marker elevation without any apparent recurrence	1

Abbreviation: SBRT = stereotactic body radiotherapy.

Of 34 patients, disease progression observed in 23 patients; 1 patient had regrowth at site of SBRT and liver metastasis simultaneously.

Table 4. Toxicity

Toxicity	Grade 0	1	2	3
Pulmonary	6	23	4	1
Skin	27	6	1	0
Pain	27	6	0	0
Musculoskeletal	32	2	0	0
Cardiac general (pericardial effusion)	32	2	0	0
Hepatobiliary	33	1	0	0

Total number of patients was 34.

observed in 2 patients (6%): bone fracture of the rib and musculitis of the chest wall. With these dermatologic or musculoskeletal complications of the thoracic wall, mild pain was observed in 6 patients (17%). Grade 1 pericardial effusion and temporal liver dysfunction were observed in 1 patient (3%) each. Most adverse events remained at Grade 1. No adverse effects of the spinal cord, great vessels, or esophagus were observed.

Prognostic factors

We also analyzed the survival differences stratified by the disease-free interval (DFI), previous chemotherapy, previous thoracic surgery, performance status, nodule size (sum of longer diameters), and number of targets. Except for DFI, no significant differences were observed. We stratified patients into three groups according to the DFI; <1 year, >1 year but <3 years, and >3 years (Fig. 3). Patients with DFI >3 years had significantly greater overall survival (p = 0.02) among the three groups. However, other factors showed negative results, which might suggest a limitation of this small group study.

DISCUSSION

Our clinical standard dose fractionation of SBRT for primary lung cancer was 48 Gy in four fractions. For metastatic lung cancer, we escalated the dose to 60 Gy because three local failures occurred with the 48-Gy dose. At last follow-up, 60 Gy appears to have been well tolerated by the patients with lung metastases. No local progression occurred with the 60-Gy dose. The difference between 48 and 60 Gy was not statistically significant in the survival rate, but was marginally significant (p = 0.078) in the local progression rate. The incidence of Grade 1 and 2 pulmonary toxicity was comparable between the two doses, with 13 (72%) and 2 (11%) at 48 Gy and 10 (63%) and 2 (13%) at 60 Gy, respectively. Dose escalation from 48 to 60 Gy increased the local control rate without increasing the incidence or severity of pulmonary toxicity.

Several reports have been published regarding the outcomes of SBRT for primary or metastatic lung tumors. Table 5 lists the survival outcomes after SBRT for pulmonary metastases in these reports. Onimaru *et al.* (8) and Wulf

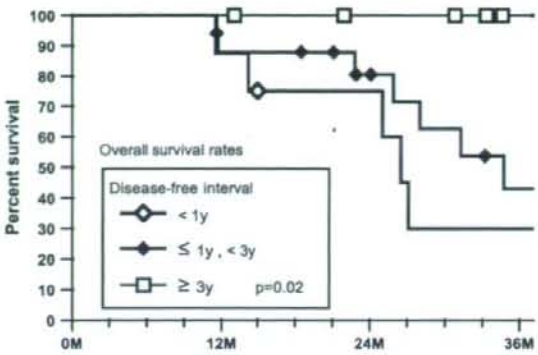

Fig. 3. Overall survival rates stratified by disease-free interval (p = 0.02).

(14) reported overall survival rates of 49% and 33% at 2 years. Lee *et al.* (7) did not report the actuarial 2-year survival rate, although we calculated the crude survival rate to be 68% from data in their summary table. In the present study, it was 84%. The biologically effective dose, assuming the α/β ratio to be 10 (BED_{10}), in the present study was 105.6 Gy and 132.0 Gy for 48 Gy in four fractions and 60 Gy in five fractions, respectively. Onishi *et al.* (15) concluded that a BED_{10} of >100 Gy at the isocenter is preferable for the treatment of primary lung cancer to achieve a better overall survival rate. The BED_{10} of SBRT for pulmonary metastases ranged from 70 to 162 Gy, and the survival rates at 2 years ranged from 33% to 84% (Table 5).

An important aspect when discussing these results is the difference in treatment planning. One is the dose prescription point. We prescribed the dose to the isocenter. In contrast, some institutes prescribed to the margin of the PTV. Second is the PTV margin. The PTV margin differs depending on the setup accuracy at each institution. Third is the PTV contour. Contouring of the PTVs would reflect a difference in CT scanning: CT scanning with free breathing vs. breath holding and slow vs. fast scan times. Fourth is the dose calculation algorithm, including the inhomogeneity correction. Differences in the dose calculation algorithm would affect the marginal dose, particularly in treatment planning for lung tumors. Thus, we prescribed the dose to the isocenter to avoid unintended dose variations. Recently, more accurate dose calculation has become common, and adoption of a prescription with respect to the PTV is also worth considering, if a standard method has been established.

Surgical pulmonary metastasectomy has been recognized as a potentially curative treatment, particularly for patients without other metastases. Our published data review revealed that the 5-year survival rate for these patients was 26–40% (21–30) (Table 6). According to the International Registry of Lung Metastases, with >5,000 cases, surgical resection for metastatic lung tumor can result in long-term survival (21). In the International Registry of Lung

Table 5. SBRT for pulmonary metastases

Investigator	Primary tumor (*n*)	Patients (*n*)	Prescription	BED_{10} @ IC	Target	2-y Survival rate (%)
Lee *et al.* (7), 2003	Lung 5, liver 3, esophagus 2, trachea 2	19	30 Gy/3 Fr to 40 Gy/4 Fr		CTV: GTV + 5 mm	68*
		12	30 Gy/3 Fr (median 90% @ PTV margin)	70†	PTV: CTV + 5–10 mm	
		7	40 Gy/4 Fr (median 90% @ PTV margin)	94†		
Onimaru *et al.* (8), 2003	Lung 6, kidney 6, breast 2	20	48 Gy/8 Fr to 60 Gy/8 Fr		ITV	49
		15	48 Gy/8 Fr @ IC	76.8	PTV: ITV + 5–10 mm	
		5	60 Gy/8 Fr @ IC	105.0		
Wulf *et al.* (14), 2004	Lung 23, breast 5, colorectum 4, kidney 4, sarcoma 4	51	26 Gy/1 Fr to 37.5 Gy/3 Fr		CTV: GTV + 2–3 mm	33
		25	26 Gy/1 Fr (80% @ PTV margin)	138†	PTV: CTV+ 5–10 mm	
		12	30 Gy/3 Fr (100% @ PTV margin, 150% @ IC)	112.5		
		5	36 Gy/3 Fr (100% @ PTV margin, 150% @ IC)	151.2		
		9	37.5 Gy/3 Fr (100% @ PTV margin, 150% @ IC)	161.7		
Present study	Lung 15, colorectum 9, head and neck 5, kidney 3	34	48 Gy/4 Fr to 60 Gy/5 Fr		ITV	84
		18	48 Gy/4 Fr @ IC	105.6	PTV: ITV + 5 mm	
		16	60 Gy/5 Fr @ IC	132.0		

Abbreviations: SBRT = stereotactic body radiotherapy; BED_{10} = biologically effective dose ($\alpha/\beta = 10$); IC = isocenter; Fr = fractions; CTV = clinical target volume; GTV = gross tumor volume; PTV = planning target volume; ITV = internal target volume.

* Calculated from patient summary table.

† Estimations according to their marginal doses.

Metastases study, with the exclusion of the apparently favorable tumors (*i.e.*, germ cell and Wilms tumors), the survival outcome at 2 years was approximately 70%. In our study, the overall survival rate at 2 years was 84%. Thus, SBRT appears to have the potential to cure, similar to that of surgical metastasectomy.

Table 6. Results of metastasectomy

Investigator	Year	Primary cancer	Patients (n)	5-y Survival rate (%)
IRLM (21)	1997	Various	4,572	36
		Epithelial tumor	1,984	
		Sarcoma	1,917	
		Germ cell tumor	318	
		Melanoma	282	
		Other	70	
van Rens *et al.* (23)	2001	Lung	121	26
Saito *et al.* (25) (KCOG)	2002	Colorectum	165	40
Pfannschmidt *et al.* (27)	2003	Colorectum	167	32

Abbreviations: IRLM = International Registry of Lung Metastases; KCOG = Kansai Clinical Oncology Group.

The International Registry of Lung Metastases also analyzed prognostic factors. They found that a DFI of ≥36 months, a single metastasis, and germ cell or Wilms tumor as the primary tumor were factors resulting in a good prognosis. In our study, a longer DFI of >3 years was also a good prognostic factor. They also showed that the difference in relative risk was not substantial for those with common epithelial cancers such as those of the bowel, breast, head and neck, and kidney. In our study, no significant difference was found in overall survival between those with metastases from lung cancer and those with metastases from other sites. For selected patients with pulmonary oligometastases, survival after SBRT might not be affected by the primary disease.

CONCLUSION

The optimal regimen of SBRT for pulmonary metastasis has not yet been determined: 60 Gy was well tolerable and was superior to 48 Gy for local control at 2 years. SBRT for oligometastatic lung tumors was comparable to surgical metastasectomy with regard to the 2-year overall survival rate. SBRT could be an effective treatment for oligometastatic lung tumors.

REFERENCES

1. Uematsu M, Shioda A, Tahara K, *et al.* Focal, high dose, and fractionated modified stereotactic radiation therapy for lung carcinoma patients: A preliminary experience. *Cancer* 1998;82: 1062–1070.
2. Nakagawa K, Aoki Y, Tago M, *et al.* Megavoltage CT-assisted stereotactic radiosurgery for thoracic tumors: Original research in the treatment of thoracic neoplasms. *Int J Radiat Oncol Biol Phys* 2000;48:449–457.
3. Wulf J, Hadinger U, Oppitz U, *et al.* Stereotactic radiotherapy of extracranial targets: CT-simulation and accuracy of treatment in the stereotactic body frame. *Radiother Oncol* 2000;57:225–236.
4. Hara R, Itami J, Kondo T, *et al.* Stereotactic single high dose irradiation of lung tumors under respiratory gating. *Radiother Oncol* 2002;63:159–163.
5. Nagata Y, Negoro Y, Aoki T, *et al.* Clinical outcomes of 3D conformal hypofractionated single high-dose radiotherapy for one or two lung tumors using a stereotactic body frame. *Int J Radiat Oncol Biol Phys* 2002;52:1041–1046.
6. Hof H, Herfarth KK, Munter M, *et al.* Stereotactic single-dose radiotherapy of stage I non-small-cell lung cancer (NSCLC). *Int J Radiat Oncol Biol Phys* 2003;56:335–341.
7. Lee SW, Choi EK, Park HJ, *et al.* Stereotactic body frame based fractionated radiosurgery on consecutive days for primary or metastatic tumors in the lung. *Lung Cancer* 2003;40:309–315.
8. Onimaru R, Shirato H, Shimizu S, *et al.* Tolerance of organs at risk in small-volume, hypofractionated, image-guided radiotherapy for primary and metastatic lung cancers. *Int J Radiat Oncol Biol Phys* 2003;56:126–135.
9. Onishi H, Kuriyama K, Komiyama T, *et al.* A new irradiation system for lung cancer combining linear accelerator, computed tomography, patient self-breath-holding, and patient-directed beam-control without respiratory monitoring devices. *Int J Radiat Oncol Biol Phys* 2003;56:14–20.
10. Singh D, Yi WS, Brasacchio RA, *et al.* Is there a favorable subset of patients with prostate cancer who develop oligometastases? *Int J Radiat Oncol Biol Phys* 2004;58:3–10.
11. Kavanagh BD, McGarry RC, Timmerman RD. Extracranial radiosurgery (stereotactic body radiation therapy) for oligometastases. *Semin Radiat Oncol* 2006;16:77–84.
12. Yang JC, Abad J, Sherry R. Treatment of oligometastases after successful immunotherapy. *Semin Radiat Oncol* 2006;16: 131–135.
13. Rubin P, Brasacchio R, Katz A. Solitary metastases: Illusion versus reality. *Semin Radiat Oncol* 2006;16:120–130.
14. Wulf J, Haedinger U, Oppitz U, *et al.* Stereotactic radiotherapy for primary lung cancer and pulmonary metastases: A noninvasive treatment approach in medically inoperable patients. *Int J Radiat Oncol Biol Phys* 2004;60:186–196.
15. Onishi H, Araki T, Shirato H, *et al.* Stereotactic hypofractionated high-dose irradiation for stage I nonsmall cell lung carcinoma: Clinical outcomes in 245 subjects in a Japanese multiinstitutional study. *Cancer* 2004;101:1623–1631.
16. Nagata Y, Takayama K, Matsuo Y, *et al.* Clinical outcomes of a phase I/II study of 48 Gy of stereotactic body radiotherapy in 4 fractions for primary lung cancer using a stereotactic body frame. *Int J Radiat Oncol Biol Phys* 2005;63: 1427–1431.
17. Zimmermann FB, Geinitz H, Schill S, *et al.* Stereotactic hypofractionated radiation therapy for stage I non-small cell lung cancer. *Lung Cancer* 2005;48:107–114.
18. Negoro Y, Nagata Y, Aoki T, *et al.* The effectiveness of an immobilization device in conformal radiotherapy for lung tumor: Reduction of respiratory tumor movement and evaluation of the daily setup accuracy. *Int J Radiat Oncol Biol Phys* 2001; 50:889–898.
19. Takayama K, Nagata Y, Negoro Y, *et al.* Treatment planning of stereotactic radiotherapy for solitary lung tumor. *Int J Radiat Oncol Biol Phys* 2005;61:1565–1571.
20. Aoki T, Nagata Y, Negoro Y, *et al.* Evaluation of lung injury after three-dimensional conformal stereotactic radiation therapy for solitary lung tumors: CT appearance. *Radiology* 2004;230: 101–108.
21. The International Registry of Lung Metastases. Long-term results of lung metastasectomy: Prognostic analyses based on 5206 cases. *J Thorac Cardiovasc Surg* 1997;113:37–49.
22. Asaph JW, Keppel JF, Handy JR Jr., *et al.* Surgery for second lung cancers. *Chest* 2000;118:1621–1625.
23. van Rens MT, Zanen P, de la Riviere AB, *et al.* Survival after resection of metachronous non-small cell lung cancer in 127 patients. *Ann Thorac Surg* 2001;71:309–313.
24. Sakamoto T, Tsubota N, Iwanaga K, *et al.* Pulmonary resection for metastases from colorectal cancer. *Chest* 2001;119: 1069–1072.
25. Saito Y, Omiya H, Kohno K, *et al.* Pulmonary metastasectomy for 165 patients with colorectal carcinoma: A prognostic assessment. *J Thorac Cardiovasc Surg* 2002;124: 1007–1013.
26. Rena O, Casadio C, Viano F, *et al.* Pulmonary resection for metastases from colorectal cancer: factors influencing prognosis: Twenty-year experience. *Eur J Cardiothorac Surg* 2002; 21:906–912.
27. Pfannschmidt J, Muley T, Hoffmann H, *et al.* Prognostic factors and survival after complete resection of pulmonary metastases from colorectal carcinoma: experiences in 167 patients. *J Thorac Cardiovasc Surg* 2003;126:732–739.
28. Inoue M, Ohta M, Iuchi K, *et al.* Benefits of surgery for patients with pulmonary metastases from colorectal carcinoma. *Ann Thorac Surg* 2004;78:238–244.
29. Monteiro A, Arce N, Bernardo J, *et al.* Surgical resection of lung metastases from epithelial tumors. *Ann Thorac Surg* 2004;77:431–437.
30. Kondo H, Okumura T, Ohde Y, *et al.* Surgical treatment for metastatic malignancies—Pulmonary metastasis: Indications and outcomes. *Int J Clin Oncol* 2005;10:81–85.

IOP PUBLISHING PHYSICS IN MEDICINE AND BIOLOGY

Phys. Med. Biol. 53 (2008) 2413–2423 doi:10.1088/0031-9155/53/9/013

Time-dependent cell disintegration kinetics in lung tumors after irradiation

Alexei V Chvetsov[1], Jatinder J Palta[1] and Yasushi Nagata[2]

[1] Department of Radiation Oncology, University of Florida, Gainesville, FL, USA
[2] Department of Therapeutic Radiology and Oncology, Kyoto University, Kyoto, Japan

E-mail: chvetsov@ufl.edu

Received 27 January 2008, in final form 17 March 2008
Published 17 April 2008
Online at stacks.iop.org/PMB/53/2413

Abstract

We study the time-dependent disintegration kinetics of tumor cells that did not survive radiotherapy treatment. To evaluate the cell disintegration rate after irradiation, we studied the volume changes of solitary lung tumors after stereotactic radiotherapy. The analysis is performed using two approximations: (1) tumor volume is a linear function of the total cell number in the tumor and (2) the cell disintegration rate is governed by the exponential decay with constant risk, which is defined by the initial cell number and a half-life $T_{1/2}$. The half-life $T_{1/2}$ is determined using the least-squares fit to the clinical data on lung tumor size variation with time after stereotactic radiotherapy. We show that the tumor volume variation after stereotactic radiotherapy of solitary lung tumors can be approximated by an exponential function. A small constant component in the volume variation does not change with time; however, this component may be the residual irregular density due to radiation fibrosis and was, therefore, subtracted from the total volume variation in our computations. Using computerized fitting of the exponent function to the clinical data for selected patients, we have determined that the average half-life $T_{1/2}$ of cell disintegration is 28.2 days for squamous cell carcinoma and 72.4 days for adenocarcinoma. This model is needed for simulating the tumor volume variation during radiotherapy, which may be important for time-dependent treatment planning of proton therapy that is sensitive to density variations.

1. Introduction

The goal of this paper is to show that the time-dependent disintegration of tumor cells which do not survive radiotherapy can be described using a simple analytical function. These cells are supposed to be lethally damaged by radiation with the probability described, for instance, by the LQ-model; however, they exist in some intact form and contribute to the tumor volume

0031-9155/08/092413+11$30.00

even though they are not able to proliferate (Fowler 1989, Hall and Giaccia 2006). We assume that these cells disintegrate at the first or subsequent division and their debris is removed from the tumor. This mechanism called mitotic death is a common form of cell death after irradiation; however, the probability of other disintegration mechanisms like apoptosis can also be included in our model (Hall and Giaccia 2006). The time-dependent kinetics which we apply to the population of lethally damaged cell has also been successfully used for the population of neurons with inherited degenerations (Clarke *et al* 2000). The neuron population with inherited degenerations is very similar to the lethally damaged tumor cells because they do not proliferate and their death initiated by a random event. For the analysis of this time-dependent cell kinetics, we utilized a clinical study on the volumetric changes of solitary lung tumors after stereotactic body radiotherapy (Aoki *et al* 2004).

The disintegration model of lethally damaged cells can be used in more complicated models which describe complete tumor cell kinetics during radiation therapy. This kinetics which includes both living and lethally damaged cells is implemented, for instance, in the computer models developed by Borkenstein *et al* (2004) and Dionysiou *et al* (2004). Potentially, these models can predict tumor volume during fractionated radiotherapy which can be important for time-dependent treatment planning because the tumor volume variation causes density variations which, in turn, can affect the prescribed dose distributions. During the last few years, several clinical studies have been published on tumor volume variation *in vivo* during fractionated radiotherapy. The data in these studies have been obtained using integrated 3D imaging techniques such as CT/linear accelerator system or tomotherapy (Barker *et al* 2004, Kupelian *et al* 2005, Siker *et al* 2006). Similar studies on tumor volume variation have been done using conventional CT scanners for treatment modalities where the integrated 3D imaging was not available, for instance proton therapy (Bucci *et al* 2007). The acquired data indicate that the physiological geometry changes in tumors and normal tissues between dose fractions can affect the dose distributions during fractionated radiotherapy, with an apparent maximum effect for lung and head and neck cancers. The research on tumor volume variation is important for intensity-modulated radiation therapy (IMRT), which provides sharp dose fall-off around the tumor (Mohan *et al* 2005). Emergent proton therapy is even more sensitive to the physiological changes because of the limited range of proton beams (Engelsman and Kooy 2005, Bucci *et al* 2007).

New models for tumor volume variation have been developed which can describe anatomical changes during fractionated radiotherapy (Seibert *et al* 2007, Chao *et al* 2007). These models are based on deformable image registration techniques or database analysis; however, they do not utilize the underlying radiobiological mechanisms. Therefore, these models cannot explain many phenomena which have been observed in tumor volume variation measurements. They lack predictive power because they do not utilize radiobiological principles. We believe that radiobiological models are necessary to explain these observed phenomena and predict tumor shrinkage based on radiobiological principles.

In the radiobiological modeling for radiotherapy treatment planning research has been primarily dedicated to developing effective dose fractionation schedules, models for tumor control probability (TCP) and normal tissue complication probability (NTCP) (Moiseenko *et al* 2005, Stewart and Li 2007). Less attention has been paid to the models for volume and mass variations during radiotherapy because it was likely not assumed that these changes could significantly affect the dose distributions and treatment outcomes. The cell loss mechanisms have been studied for growing tumors to explain the difference between the potential doubling time and volume doubling time (Fowler 1991); however, the problems of quantitative evaluation of dosimetry due to volume and mass variation in treatment planning have not been addressed. Circumstances have changed recently with the invention and widespread use

of effective imaging technologies which allow monitoring of human tumors *in vivo* (Barker *et al* 2004, Kupelian *et al* 2005, Siker *et al* 2006). Volumetric radiobiological tumor response to irradiation with X-rays has been studied in animal experiments (Tannock and Howes 1973, Bernheim *et al* 1977, Spang-Thomsen *et al* 1981). The obtained data have been important for understanding the radiobiological mechanisms responsible for tumor regression; however, they cannot be applied directly to the human tumors irradiated *in vivo*. The data required for *in vivo* verification of tumor volume modeling are available now due to 3D integrated imaging technologies for monitoring the tumor volume variation during radiotherapy treatment.

In this paper, we propose a simple radiobiological model for cell disintegration kinetics after radiation damage. We believe that this model can motivate further development of the computationally efficient and practical models that describe cell kinetics and tumor-volume changes during radiotherapy. These models can potentially be used to improve time-dependent treatment planning.

2. Methods

2.1. Cell survival, death and disintegration

Irradiation of the tumor cell population with dose D causes the death of a fraction of cells. The survival process of living cells can be described using the linear-quadratic (LQ) model which is given by

$$S = \exp(-\alpha D - \beta D^2), \tag{1}$$

where α and β are the parameters of the survival model (Fowler 1989, Hall and Giaccia 2006). The survival curve S defines the relative number of cells which survive; therefore, the relative number of cells which are lethally damaged by radiation is given by $1-S$. Usually, the number of surviving clonogens is studied in treatment planning because they finally define the TCP. In this paper, we study the clonogens which did not survive irradiation because we believe that the kinetics of these clonogens defines the tumor volume variation during radiotherapy. The clonogens which are lethally damaged by radiation do not disappear instantly. They contribute to the tumor volume for a period of time until they disintegrate and their debris is removed from the tumor. This kinetics of cell loss can help us to evaluate the time-dependent tumor volume variation which, in turn, can affect the dose distributions.

It is difficult to derive the cell disintegration kinetics using the data on tumor-volume variation during radiotherapy because the tumor volume is defined by the kinetics of proliferating and damaged cells. However, after radiotherapy, we can assume that the entire cell population did not survive irradiation and is lethally damaged; therefore, we have only one cell subpopulation which is much easier to model. The clinical data on the tumor-volume variation after radiotherapy are available, for instance, for solitary lung tumors treated with stereotactic body radiotherapy (Aoki *et al* 2004).

2.2. Cell disintegration model

It is usually assumed that a cell damaged by radiation disintegrates at the first or a subsequent division after radiation damage at the dose levels used in therapy. During the time from radiation damage to disintegration, the damaged cells contribute to the tumor volume even though they are not able to proliferate. We assume that the cell disintegration rate is proportional to the number of intact damaged cells; therefore, we can write the following

differential equation for the time-dependent number of damaged cells:

$$\frac{dN(t)}{dt} = -\mu(t)N(t). \tag{2}$$

We further introduce an approximation of constant disintegration risk which assumes that the disintegration constant is time independent $\mu(t) = \mu_0$. Equation (2) with $\mu(t) = \mu_0$ has an analytical exponential decay solution which is given by

$$N(t) = N(t_0)\exp(-\mu_0 t), \tag{3}$$

where $N(t_0)$ is the number of dead intact cells at the initial time t_0. This approach is similar to the mathematical formalism used by Clarke *et al* (2000) to describe the time-dependent kinetics of cell death in inherited neuronal degenerations.

Similar to the formula for radioactive decay, we introduce a parameter called half-life for the biological decay of the damaged cell population. The half-life is defined as the time required for the number of damaged cells to decay to half of their initial value. The half-life of the damaged cell population is related to the decay constant μ_0 as

$$T_{1/2} = \frac{\ln 2}{\mu_0}. \tag{4}$$

The key problem for practical applications of this approach is to evaluate the half-life of the population of damaged cells. We have already mentioned that damaged cells disintegrate at the first attempted division; therefore, the disintegration rate may be associated with the proliferation rate because both parameters are related to the cell cycle. It is convenient to assume that the half-life $T_{1/2}$ is linearly related to the potential doubling time T_{pot} as

$$T_{1/2} = bT_{pot}, \qquad b > \ln 2. \tag{5}$$

If we take into account that the cell disintegration happens at the first or subsequent division, we can further establish that $T_{1/2} > \ln 2T_{pot}$, which allows for the parameter $b > \ln 2$. We have utilized here the relationship $T_{1/2} = \ln 2T_a$ between the half-life $T_{1/2}$ and the mean life T_a. Obviously, we have $T_a = T_{pot}$ if all damaged cells would disintegrate at the first division. For more detailed evaluation of the half-life $T_{1/2}$, we have to study the variation with time of a large population of damaged cells *in vivo*. The large population of damaged cells can be found, for instance, at the end of radiotherapy treatment where the entire population of cancer cells is assumed to have not survived irradiation.

2.3. Tumor volume simulation

One of the possible ways to study the kinetics of cell disintegration is to evaluate the tumor volume after radiotherapy because we can assume that the entire tumor cell population did not survive radiotherapy. This is a relatively simple mathematical problem because we have to evaluate only one cell subpopulation damaged by radiation and unable to proliferate. However, to evaluate the kinetics of cell disintegration based on the volumetric measurements, we have to assume a linear relationship between the tumor volume $V(t)$ and the cell number $N(t)$:

$$V(t) = vN(t), \tag{6}$$

where v is a constant which includes the cell volume and the volume of the related intercellular space. Experiments with animal irradiation indicate that the mean cell concentration in tumors can be a function of delivered radiation dose and time. Therefore, the gross changes in the tumor volume after irradiation are not always a reliable indicator of microscopic changes in the cell number. However, the experimental data of Tannock and Howes indicate that the mean cell concentration returns to the near-normal values after a limited time between 1 and 7 days

(Tannock and Howes 1973). For instance, Tannock and Howes have measured a 75% reduction in the mean cell concentration after 6 Gy with 1 day of recovery time and a 50% reduction in the mean cell concentration after 30 Gy with 7 days of recovery time. Therefore, we believe that the linear relationship between the cell number and the tumor volume is a reasonable approximation for tumor volume simulation in the clinical study analyzed in this paper. In this clinical study, tumors have been monitored during several months after radiotherapy.

3. Results

3.1. Clinical data analysis

To validate the exponential model and determine decay parameters, we used the clinical data on tumor size variation after stereotactic body radiotherapy published by Aoki *et al* (2004). This clinical study includes analysis of shrinkage of solitary lung tumors in 31 patients after administering a total dose of 48 Gy in four fractions using conformal stereotactic radiation therapy. Taking into account the survival fraction given by equation (1), we can assume that the entire cell population tumors did not survive the radiotherapy for the majority of patients at this dose; therefore, the tumor volume variation after radiotherapy should be defined by the disintegration and removal of damaged cells which are not able to proliferate. This is probably true for most of the patients because tumor control was not obtained in only two cases.

The tumor size variation with time was determined by taking CT images after radiotherapy. The relative variation of tumor size as a function of time is shown in figure 1(a) for three representative cases. Additionally, we show in figure 1(a) an exponent function with $T_{1/2} =$ 21 days. We see that the exponent function approximates the general trend in tumor size variation with time. However, the difference is that the exponent function approaches zero and the tumor volume variation approaches some constant value.

We note that the tumor size in the clinical study has been measured using the largest transversal cross section A of the tumor. To evaluate the tumor volume variation, we computed the relative change of value $AA^{1/2}$ which presents the relative volumetric change under the assumption of uniform tumor shrinkage. The relative change of the value $AA^{1/2}$ is shown in figure 1(b). We see that the constant component was reduced when the data have been recalculated to the volumetric tumor change. This small constant component in the volume variation does not change with time; therefore, this component may be due to residual irregular density as radiation fibrosis and was, therefore, subtracted from volume variation in our computations.

3.2. Evaluation of half-life and average life

To determine the half-life $T_{1/2}$ of exponential decay, we performed a computerized fitting of the exponent function to the clinical data for seven adenocarcinoma and seven squamous cell carcinoma (SCC) patients. The clinical study of Aoki *et al* includes 15 adenocarcinoma cases, 9 SCC cases, 4 metastasis cases, 2 unknown cases and 1 small cell carcinoma case. We have separated the adenocarcinoma and SCC cases and excluded all other cases. The tumor shrinkage was observed in all adenocarcinoma and SCC patients; however, not all of them had enough tumor size measurements to perform a reasonable fitting. Therefore, the patients for the fitting have been selected based on the number and density of tumor measurements available for each case. One of our selection criteria was the availability of at least three tumor measurements for each patient and at least one tumor measurement within the first 4 months after treatment.

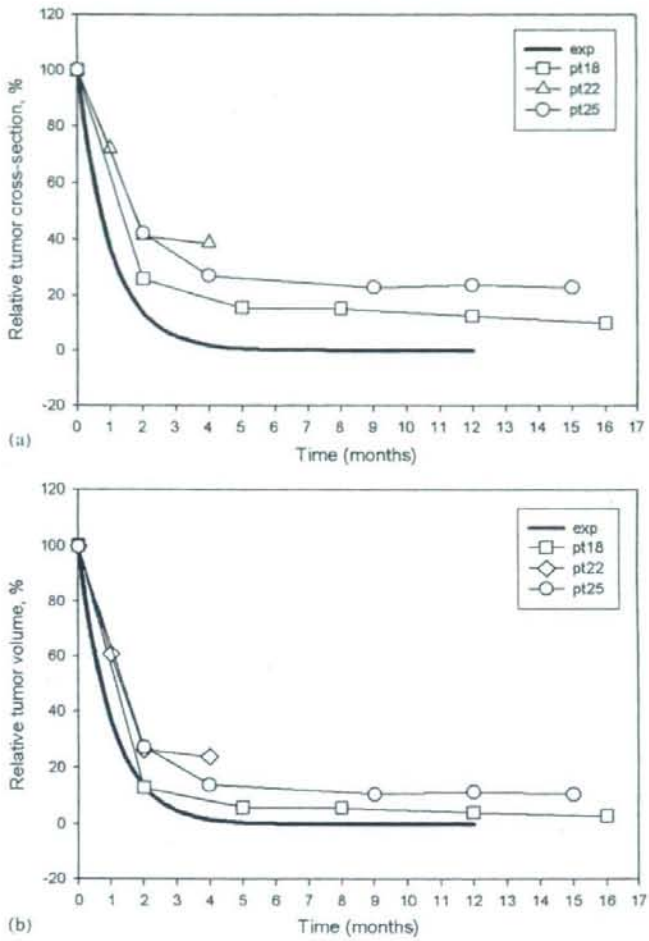

Figure 1. Comparison of relative tumor size variation after stereotactic body radiotherapy of lung as measured by Aoki *et al* with an exponent function $\exp(-t)$. (a) Clinical data for largest tumor cross-section; (b) approximation of clinical data to tumor volume.

The fitting of the exponential function was done using the least-squares minimization based on a version of a quasi-Newton method called the L-BFGB-B algorithm (Byrd *et al* 1995). This code is widely used in the medical physics community for solving different radiotherapy optimization problems of different complexity (Chvetsov *et al* 2007). The mathematical function which has been used for the fitting has been presented as a weighted linear combination of an exponent function and a constant function

$$f(t) = (1 - w)\exp(-\mu_0 t) + w, \tag{7}$$

where w is a constant value between 0.0 and 1.0. This has been done to subtract the constant saturation value in the clinical data during the optimization process.

The results of the fitting are shown in figure 2 for adenocarcinoma and in figure 3 for SCC. We have obtained the average value of half-life $T_{1/2} = 28.2$ days and standard deviation $\sigma = 8.6$ days for SCC and the average value of half-life $T_{1/2} = 72.4$ days and standard

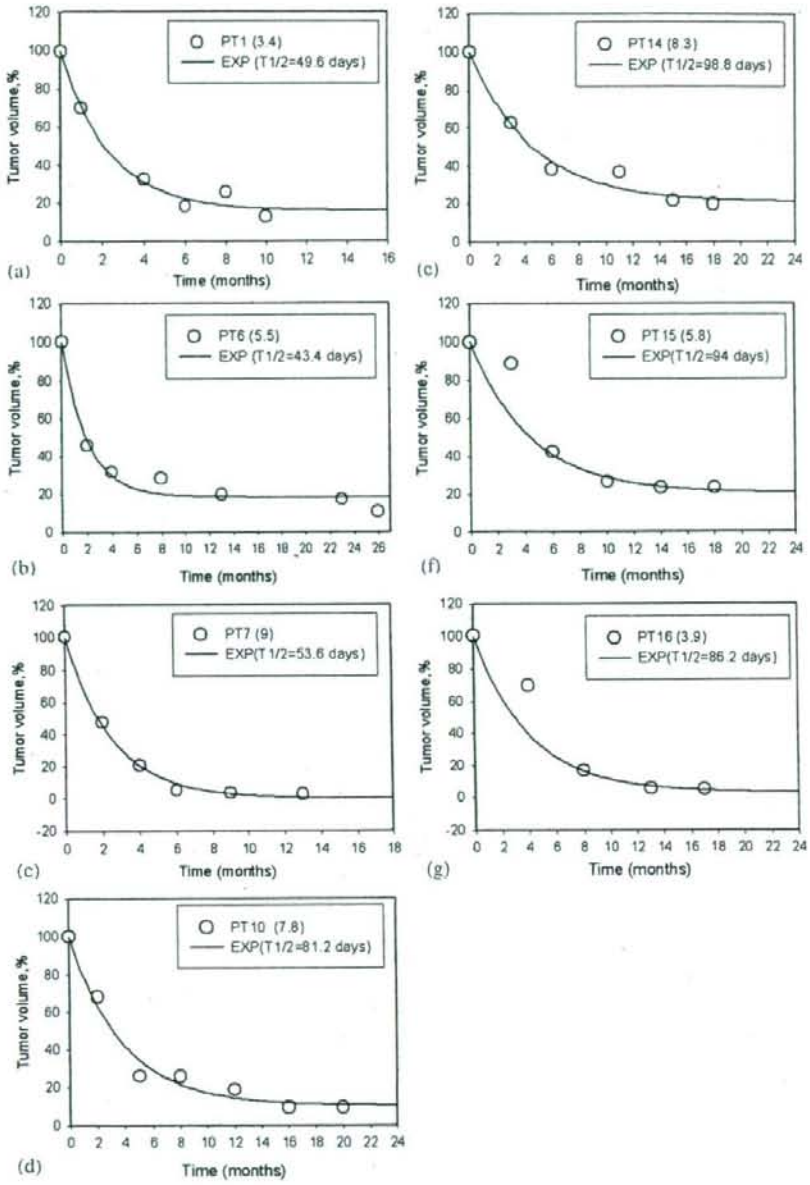

Figure 2. Comparison of the lung adenocarcinoma volume after stereotactic body radiotherapy in clinical data of Aoki *et al* with the function $(1-w)\exp(-\ln 2t/T_{1/2})+w$: (a)–(g) patients 1–7. Tumor size (cm^2) is shown for each patient in parentheses.

deviation $\sigma = 22.8$ days for adenocarcinoma. Assuming that the potential doubling time T_{pot} is 7.7 days for adenocarcinoma and 8.5 days for SCC according to the data published by Shibamoto and Hara (2005), we obtain the average value of the disintegration parameter $b = 9.4$ for adenocarcinoma and $b = 3.3$ for SCC. These data indicate that an adenocarcinoma cell cycling approximately three times longer after lethal radiation damage than a SCC cell before it disintegrates. Using the half-life we can also evaluate the mean life of a single cell if

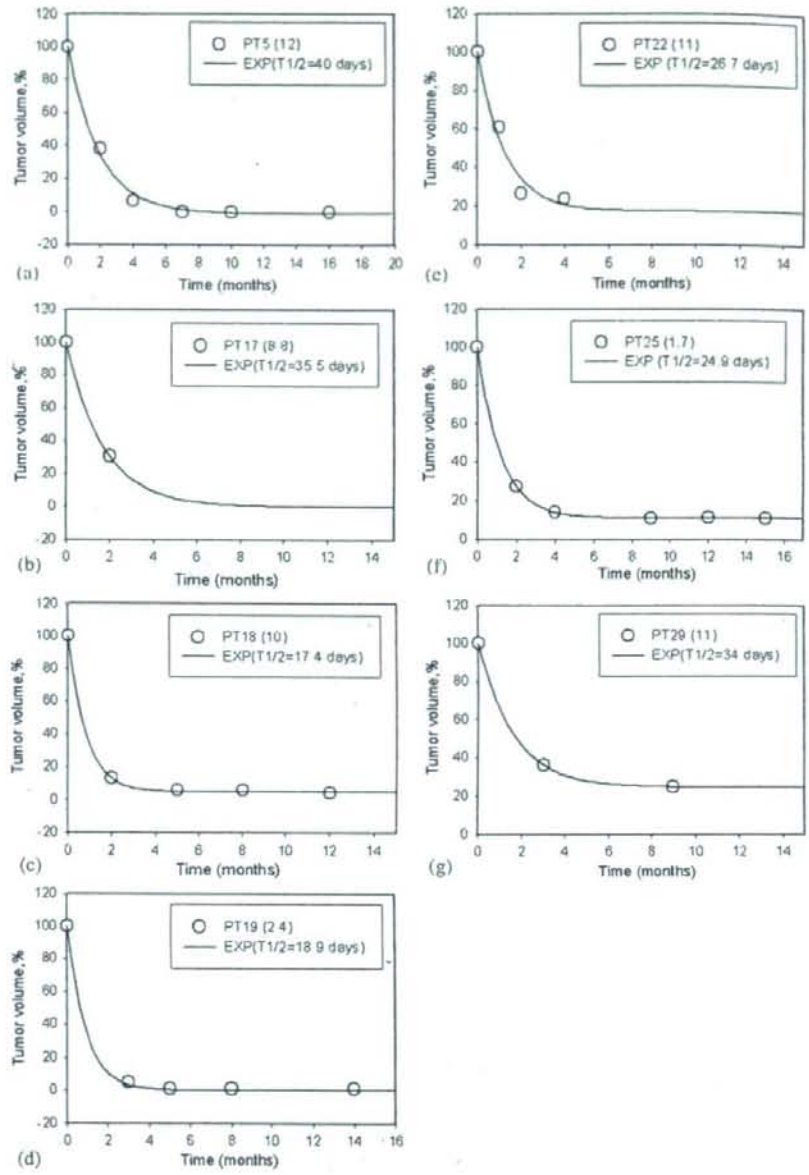

Figure 3. Comparison of the lung squamous cell carcinoma volume after stereotactic body radiotherapy in clinical data of Aoki *et al* with the function $(1-w)\exp(-\ln 2t/T_{1/2})+w$: (a)–(g) patients 1–7. Tumor size (cm^2) is shown for each patient in parentheses.

it suffers radiation damage. The mean life is given by $T_a = T_{1/2}/\ln 2$; therefore, we obtain the average mean life of $T_a = 40.7$ days for SCC and $T_a = 105.5$ days for adenocarcinoma.

The standard deviation of the half-life for both adenocarcinoma and SCC is approximately 30% of the average value. This relatively large value can be explained by several reasons: (1) patient heterogeneity is usually a reason of large standard deviation of radiobiological parameters (Wigg 2001, Keall and Webb 2007); (2) small number of cases in our evaluation

and (3) lung tumors may not be completely reoxygenated at the end of SBRT because this treatment is relatively short; therefore, lethally damaged oxygenated and hypoxic cells may be present in tumors. Hypoxic cells are practically removed from the dividing population of cells in the tumor because they are resting in the Go phase. Hypoxic cells can remain in Go phase for days, weeks or years, but can be stimulated to return to the cell division cycle. Therefore, the disintegration of lethally hypoxic cells may depend on tumor reoxygenation rate and the residual tumor hypoxia may affect heterogeneity of the measured half-life value. According to the data of Rasey *et al* (1996) obtained using PET fluoromisonidazole, the hypoxia for non-small lung cancer can be relatively large with the median value of 47.6% and the maximum value of 94.7%.

4. Discussion

In this paper, we attempted to study the kinetics of the disintegration of tumor cells damaged by radiation and, therefore, unable to proliferate. The radiobiological analysis for radiotherapy treatment planning usually involves the kinetics of proliferating cells because they define the optimal fractionation schedules and treatment outcomes given by TCP and NTCP (Moiseenko *et al* 2005, Stewart and Li 2007). In this radiobiological analysis, a cell is considered instantaneously gone from the system if it is lethally damaged by radiation.

However, the development of new imaging systems has led to more evidence that volumetric tumor changes during radiotherapy can affect tumor dosimetry in highly conformal therapies like proton therapy (Bucci *et al* 2007). Volumetric tumor changes are defined by both proliferating cells and lethally damaged cells which are not able to proliferate. Lethally damaged cells will disintegrate with time and their kinetics will affect the dynamics of tumor mass and volume. The cell loss mechanism has been addressed in the studies discussing tumor growth and its relationship to the potential doubling time and volume doubling time (Fowler 1991). However, quantitative modeling of the tumor volume variation during or after radiotherapy has not been emphasized in radiotherapy treatment planning.

Modeling the volumetric tumor response is a complicated mathematical and radiobiological task because several cell subpopulations should be considered, including proliferating and damaged cells. Many radiobiological processes such as cell survival, reoxygenation, repopulation and reassortment should be modeled. Therefore, we began with the simple task of modeling with a tumor with only one subpopulation, which could be found at the end of the radiotherapy treatment after all living cells were destroyed by ionizing radiation. The tumor at the end of the therapy consisted only of the population of damaged cells which could not proliferate; however, they did make up the bulk of the tumor. These cells disintegrate at the first or a subsequent division after irradiation and their debris is removed.

In this study, we proposed and validated a simple mathematical formula for cell disintegration in tumors treated with ionizing radiation. The parameters of the model have been obtained using clinical data on tumor size variation after stereotactic radiotherapy of solitary lung tumors. To study the cell kinetics based on the volumetric measures, we assumed a linear relationship between the cell number and the tumor volume. We have shown that many complicated processes such as mitotic cell death and diffusion of cell debris can be described as a simple exponential decay. We believe that this model can lead to further development of a fast computational radiobiological model to predict the tumor volume variation during fractionated radiotherapy. To simulate tumor volume during radiotherapy, this model should additionally include an analysis of subpopulations of live cells governed by radiobiological mechanisms such as the LQ survival model, exponential repopulation, reoxygenation and reassortment.

We believe that a radiobiological model for volumetric tumor response is needed for qualitative and quantitative analyses of the most recent clinical results on anatomical changes in the human body during radiation therapy (Barker *et al* 2004, Kupelian *et al* 2005, Siker *et al* 2006, Bucci *et al* 2007). These clinical results indicate that volumetric tumor changes during radiotherapy can affect treatment planning dosimetry for highly conformal radiotherapeutic modalities like IMRT and proton beams. The radiobiological model for volumetric tumor variation can be used in 4D treatment planning for evaluating dose distribution variations which may be due to time-dependent density variations in highly conformal radiotherapeutic modalities like IMRT and proton therapy (Mohan *et al* 2005). The cell disintegration model which we have proposed in this paper can be used in more complicated models for tumor volumetric response during radiotherapy which should include kinetics of living and lethally damaged cells. If these models would be developed they would allow one evaluate dose variations due to time-dependent density variations thus improving 4D treatment planning. The ability to model tumor volume during radiotherapy can especially improve and optimize 4D treatment planning for IMRT and proton therapy, which is a laborious and time-consuming process.

Acknowledgments

This research was partially supported by an Elekta research grant. The authors would like to thank Dr D Siemann and Dr W M Mendenhall for valuable discussions about tumor radiobiology.

References

Aoki T, Nagata Y, Negoro Y, Takayama K, Mizowaki T, Kokubo M, Oya N, Mitsumori M and Hiraoka M 2004 Evaluation of lung injury after three-dimensional conformal stereotactic radiation therapy for solitary lung tumors: CT appearance *Radiology* **230** 101–8

Barker J L *et al* 2004 Quantification of volumetric and geometric changes occurring during fractionated radiotherapy for head-and-neck cancer using an integrated CT/linear accelerator system *Int. J. Radiat. Oncol. Biol. Phys.* **59** 960–70

Bernheim J L, Mendelsohn J, Kelly M F and Dorian R 1977 Kinetics of cell death and disintegration in human lymphocyte cultures *Proc. Natl. Acad. Sci. USA* **74** 2536–40

Borkenstein K, Levegrün S and Peschke P 2004 Modeling and computer simulations of tumor growth and tumor response to radiation therapy *Rad. Res.* **162** 71–83

Bucci M K, Dong L, Liao Z, Chang J, Cox J, Komaki R, Gillin M and Mohan R 2007 Comparison of tumor shrinkage in proton and photon radiotherapy of lung cancer *Int. J. Radiat. Oncol. Biol. Phys.* **63** S686–S7

Byrd R H, Lu P, Nocedal J and Zhu C 1995 A limited memory algorithm for bound constrained optimization *SIAM J. Sci. Comput.* **16** 1190–1208

Chao M, Xie Y, Le Q and Xing L 2007 Modeling the volumetric change of head and neck tumor in response to radiation therapy *Int. J. Radiat. Oncol. Biol. Phys.* **69** S741 (abstract)

Chvetsov A V, Dempsey J F and Palta J R 2007 Optimization of equivalent uniform dose using the L-curve criterion *Phys. Med. Biol.* **52** 5973–84

Clarke G, Collins R A, Leavitt B R, Andrews D F, Hayden M R, Lumsten C J and Mcinnes R R 2000 A one-hit model of cell death in inherited neuronal degenerations *Nature* **406** 195–9

Dionysiou D D, Stamatakos G S, Uzunoglu N K, Nikita K S and Marioli A 2004 A four-dimensional simulation model of tumor response to radiotherapy *in vivo*: parametric validation considering radiosensitivity, genetic profile and fractionation *J. Theor. Biol.* **230** 1–20

Engelsman M and Kooy H M 2005 Target volume dose considerations in proton beam treatment planning for lung tumors *Med. Phys.* **32** 3549–57

Fowler J F 1989 The linear-quadratic formula and progress in fractionated radiotherapy *Br. J. Radiol.* **62** 679–4

Fowler J F 1991 The phantom of tumor treatment—continually rapid proliferation unmasked *Radiother. Oncol.* **22** 156–8

Hall E J and Giaccia A J 2006 *Radiobiology for the Radiologist* 6th edn (Philadelphia: Lippincott, Williams & Wilkins)

Keall P J and Webb S 2007 Optimum parameters in a model for tumor control probability, including interpatient heterogeneity: evaluation of the log-normal distribution *Phys. Med. Biol.* **52** 291–302

Kupelian P A, Ramsey C, Meeks S L, Willoughby T R, Forbes A, Wagner T H and Langen K M 2005 Serial megavoltage CT imaging during external beam radiotherapy for non-small-cell lung cancer: observations on tumor regression during treatment *Int. J. Radiat. Oncol. Biol. Phys.* **63** 1024–28

Mohan R, Zhang X, Wang H, Kang Y, Wang X, Liu H, Ang K K, Kuban D and Dong L 2005 Use of deformed intensity distribution for on-line modification of image-guided IMRT to account for interfractional anatomic changes *Int. J. Radiat. Oncol. Biol. Phys.* **61** 1258–66

Moiseenko V, Deasy J O and Van DyK J 2005 Radiobiological modeling for treatment planning *The Modern Technology of Radiation Oncology. A Compendium for Medical Physicists and Radiation Oncologists* vol 2 ed J Van Dyk (Madison, WI: Medical Physics Publishing) pp 185–220

Rasey J S, Koh W J, Evans M L, Peterson L M, Lewellen T K, Graham M M and Kronh K A 1996 Quantifying regional hypoxia in human tumors with positron emission tomography of [^{18}F] fluoromisonidazole: a pretherapy study of 37 patients *Int. J. Radiat. Oncol. Biol. Phys.* **36** 417–28

Seibert R M, Ramsey C R, Hines J W, Kupelian P A, Langen K M, Meeks S L and Scaperoth D D 2007 A model for predicting lung cancer response to therapy *Int. J. Radiat. Oncol. Biol. Phys.* **67** 601–9

Shibamoto Y and Hara M 2005 Radiobiology of normal lung tissue and lung tumors *Advances in Radiation Oncology in Lung Cancer* ed B Jeremić (Berlin: Springer) pp 59–66

Siker M L, Tome W A and Metha M P 2006 Tumor volume changes on serial imaging with megavoltage CT for non-small-cell lung cancer during intensity modulated radiotherapy: how reliable, consistent, and meaningful is the effect? *Int. J. Radiat. Oncol. Biol. Phys.* **66** 135–41

Spang-Thomsen M, Visfeldt J and Nielsen A 1981 Effect of single-dose X radiation on the growth curves of a human malignant melanoma transplanted into nude mice *Radiat. Res.* **85** 184–95

Stewart R D and Li X A 2007 BGRT: biologically guided radiation therapy—the future is fast approaching! *Med. Phys.* **34** 3739–51

Tannock I and Howes A 1973 The response of viable tumor cords to a single dose of radiation *Radiat. Res.* **55** 477–86

Wigg D R 2001 *Applied Radiobiology and Bioeffect Planning* (Madison, WI: Medical Physics Publishing)

肺癌
―照射野決定のための画像診断のポイントと効果判定・経過観察の注意点―

永田 靖*,** 澁谷景子* 松尾幸憲* 山内智香子*
小倉健吾* 平岡真寛*

肺癌の病期診断では，正確なTNM分類を行うために，肺内小腫瘤，脳内小腫瘤，副腎内腫瘤，骨腫瘤，リンパ節の診断が重要である．また，治療効果判定においては腫瘍の最大縮小時期の見極めが，再発判定においては放射線肺臓炎と残存腫瘤との鑑別が重要である．

はじめに

“放射線治療のための画像診断”とは，言い換えると“放射線治療医の求める画像診断レポート”と言えよう．そして“放射線治療に必要な画像診断”とは，1) 正確な病期診断，2) 適切な治療効果判定，3) 迅速な再発診断の3点に集約できよう．

一般に画像診断は大きく分けて，

1) 存在診断（病気があるかないか?）
2) 性状診断（悪性か良性か?）
3) 進展診断（どこまで病気が進展しているか?）

に分類できる．このなかで，放射線治療において大部分は，既に癌であることが組織学的に確定している疾患や病変を治療対象としているために，上記の3) の進展診断が最も重要である．しかし，後述する理由により，2) の性状診断もまた非常に重要である．また，放射線治療は，最大効果出現の時期が疾患や部位，組織型により異なる．そのために，適切な時期に最適な画像診断法で効果判定を行うことが重要である．これに密接に関連して，放射線治療後の残存瘢痕と再発診断が臨床上では非常に重要となる．

本稿では，肺癌に特化して以上の項目について検討したい．

肺癌は，年間約3万人の患者が放射線治療を受け，放射線治療対象のなかで最も多い疾患のひとつである．このなかにはI期早期肺癌に対する定位（ピンポイント）放射線照射[1]，II～III期肺癌に対する根治的化学放射線治療，IV期肺癌（骨転移，肺転移，上大静脈症候群）に対する緩和照射が含まれる．

1. 正確な病期診断

まず，病変がどこまで進展しているかによって治療方針が大きく異なる．これを規定するものがいわゆるTNM分類である．治療前に正確なTNM分類が行われて初めて最適な治療法の選択が可能となる．

肺癌のTNM分類は，表に示すとおりである．

T分類において，現在は腫瘍サイズが最大径3cmあるかないかでT1とT2とが区別されている．しかし，2009年の国際対癌連合（UICC）のTNM分類の大改訂では，2cm，3cm，5cm，7cmでT分類が変わることになる予定である[2]．

また，T分類においては主病変以外の組織未定の肺野の小結節評価が非常に重要である．肺野の単発病変ともう1か所病変があることによって，これを転

* Nagata Y., Shibuya K., Matsuo Y., Yamauchi C., Ogura K., Hiraoka M. 京都大学医学部放射線治療科 **現）広島大学病院放射線治療部

表　肺癌のTNM分類

原発腫瘍（T）
T1：腫瘍の最大径は3.0cmまたはそれ未満の大きさで，肺または臓側胸膜に囲まれており，気管支鏡検査で浸潤が葉気管支より中枢側に及ばない．
T2：腫瘍の大きさや進展度が以下のいずれかのもの．
最大径が3cmを超えるもの．
主気管支に浸潤し，気管分岐部より2.0cmあるいはそれより末梢にある．
臓側胸膜に浸潤．
肺門に及ぶが片肺全野には及ばない無気肺あるいは閉塞性肺臓炎に関連する．
T3：大きさと無関係に隣接臓器，すなわち胸壁［肺尖部胸壁浸潤肺癌（superior sulcus tumor）を含む］，横隔膜，縦隔胸膜，壁側心膜などに直接浸潤する腫瘍．腫瘍の中枢側が気管分岐部より2.0cm未満に及ぶが，気管分岐部に浸潤のないもの．また，無気肺・閉塞性肺臓炎が片肺全野に及ぶもの．
T4：大きさと無関係に次のどれかに浸潤の及ぶ腫瘍．
縦隔，心臓，大血管，気管，食道，椎体，気管分岐部．
あるいは同一肺葉内の離れた腫瘍．
あるいは悪性胸水を伴う腫瘍．

所属リンパ節（N）
N0：所属リンパ節に転移がない．
N1：同側気管支周囲と同側肺門リンパ節転移の少なくとも一方，そして肺腫瘍の直接進展を含む肺内リンパ節転移．
N2：同側縦隔と気管分岐部リンパ節転移の少なくとも一方．
N3：対側縦隔，対側肺門，同側または対側の斜角筋前，あるいは鎖骨上リンパ節転移．

遠隔転移（M）
M0：遠隔転移がない．
M1：遠隔転移がある．

移とすれば，T1がT4ないしはM1に大きく変化することになる．もし，これが肉芽腫ならT1N0M0のままである．つまり，根治の望めるT1N0M0ならば手術や体幹部定位照射が可能である．しかし，T1N0M1では化学療法か緩和医療の対象となり，治療方針が大きく異なることになる．以上の点より，画像診断レポート作成時に組織診断の確定していない肺野の小結節については，診断に注意が必要である．明確な根拠なしに肺内転移と診断すると，患者が治癒のチャンスを失う可能性があるためである．図1は，組織診断のつかなかった次第に拡大する肺腫瘤の1例である．

また，現在の保険診療上で，肺転移腫瘍に対して3か所以内なら定位放射線照射が適応となる．仮に，4か所以上の腫瘍なら化学療法の対象となる．腫瘍が3個か4個かで大きく治療方針が異なってくる事例である．肺野の小腫瘤の診断が治療方針に大きく影響し，画像診断レポートにおいて「多発転移」のみでは，臨床判断には不十分な理由である．

T分類において壁側胸膜に浸潤しているかについては，4次元動画CTも有用である．

次にN分類におけるリンパ節転移についても，癌

CT（肺野条件）

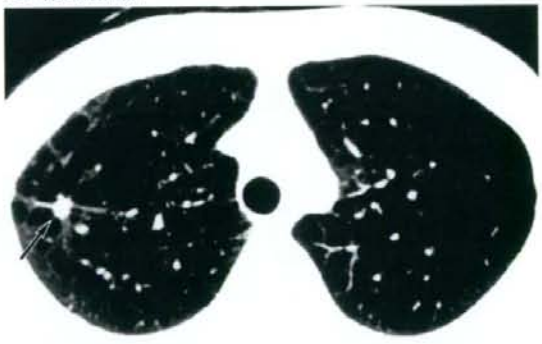

図1　組織型の確認できなかった次第に拡大してくる孤立性肺腫瘤
臨床的に肺癌とされ体幹部定位照射が行われた（→）．

の転移以外に炎症性腫脹やサルコイド反応（図2）があることは言うまでもない．サルコイド反応であっても照射でリンパ節は縮小する．最終的には縦隔鏡で確定しなければ，縦隔リンパ節転移の確定は難しい．

最後にM分類について検討すると，図3は左副腎に単発性の肺癌転移が疑われた症例であるが，最終